Available online at www.sciencedirect.com
ScienceDirect
Ceramics International 35 (2009) 3365–3369
CERAMICS INTERNATIONAL
www.elsevier.com/locate/ceramint

Thermal shock resistance of in situ formed Si_2N_2O–Si_3N_4 composites by gelcasting

Pei Yuchen [a], Li Shuqin [b,*], Yu Changqing [b], Huang zhengyu [b], Ma jingtao [c], Li Jialu [a]

[a] Composite Research Institute, Tianjin Polytechnic University, Tianjin, 300160, PR China
[b] Institute of 306th, China Aerospace Science and Industry Corporation, Beijing, 7203#-21, 100074, PR China
[c] Institute of Nuclear and New Energy Technology, Tsinghua University, Beijing, 100084, PR China

Received 26 November 2008; received in revised form 21 April 2009; accepted 28 May 2009
Available online 7 July 2009

Abstract

Thermal shock resistance of Si_2N_2O–Si_3N_4 composites was evaluated by water quenching and subsequent three-point bending tests of strength diminution. Si_2N_2O–Si_3N_4 composites which was prepared with in situ liquid pressureless sintering process using Yb_2O_3 and Al_2O_3 powders as sintering additives by gelcasting showed no macroscopic cracks and the critical temperature difference (ΔT_c) could be up to 1400 °C. A mass of pores existed in the sintered body and the irregular shaped fibers extended from the pores increased the thermal shock property.

Keywords: C. Thermal shock resistance; In situ reaction; Si_2N_2O–Si_3N_4

1. Introduction

Silicon nitride (Si_3N_4) ceramics is a suitable material for high temperature missile radome application because of high temperature mechanical strength, good resistance to rain erosion, low dielectric constant and loss, good thermomechanical property [1–9]. However, monolithic Si_3N_4 shows catastrophic drops in flexural strength after thermal shock above the critical temperature which cumbered the application. On the other hand, the silicon oxynitride (Si_2N_2O) ceramics have been recognized as a promising material for high temperature applications due to their good resistant to oxidation and to thermal shock [10,11]. Moreover, the results show that properly dispersed Si_2N_2O in Si_3N_4 based ceramics can optimize the properties [12]. Therefore, Si_2N_2O–Si_3N_4 ceramics were fabricated with in situ liquid pressureless sintering process using Yb_2O_3 and Al_2O_3 powders as sintering additives by gelcasting in the present work. Although the thermal shock property is very important for radome application, no research has been done on thermal shock resistance of Si_2N_2O–Si_3N_4 ceramics. So, the thermal shock resistance of Si_2N_2O–Si_3N_4 ceramics with temperature difference ranging from 500 to 1400 °C, by measuring the flexural strength of the specimen.

2. Experimental procedure

2.1. Raw materials

As starting materials, the Si_3N_4 powder (Beijing Tsinghua Unisp Lendor High Technology Ceramics Co., China, d_{50} = 0.5 μm, α phase 93%), the SiO_2 (Chengdu Sinuowei Co., Ltd., China, d_{50} = 2 μm, purify 99.95%) and sintering additives (Yb_2O_3 and Al_2O_3, Yb_2O_3 Griem Advanced Materials Co., Ltd., d_{50} = 3.5 μm, purify 99.95%, Al_2O_3 Zibo Hengji Tianli Co., Ltd., China, d_{50} = 1.56 μm, purify 99.99%). The microstructures of Si_3N_4, SiO_2, Yb_2O_3 and Al_2O_3 are shown in Fig. 1. Raw materials for the mixed AM-MBAM system are listed in Table 1.

2.2. Billet fabrication

The schematic forming process of gelcasting is described in Fig. 2. First, the mixture powder of 80 wt.% α-Si_3N_4, 10 wt.% SiO_2, 6 wt.% Yb_2O_3 and 4 wt.% Al_2O_3 powder and 0.25 wt.% dispersant were added to premix solution of organic monomer

* Corresponding author. Tel.: +86 10 88534128; fax: +86 10 88534479.
E-mail address: lishuqin97@sina.com (L. Shuqin).

0272-8842/$36.00
doi:10.1016/j.ceramint.2009.05.037

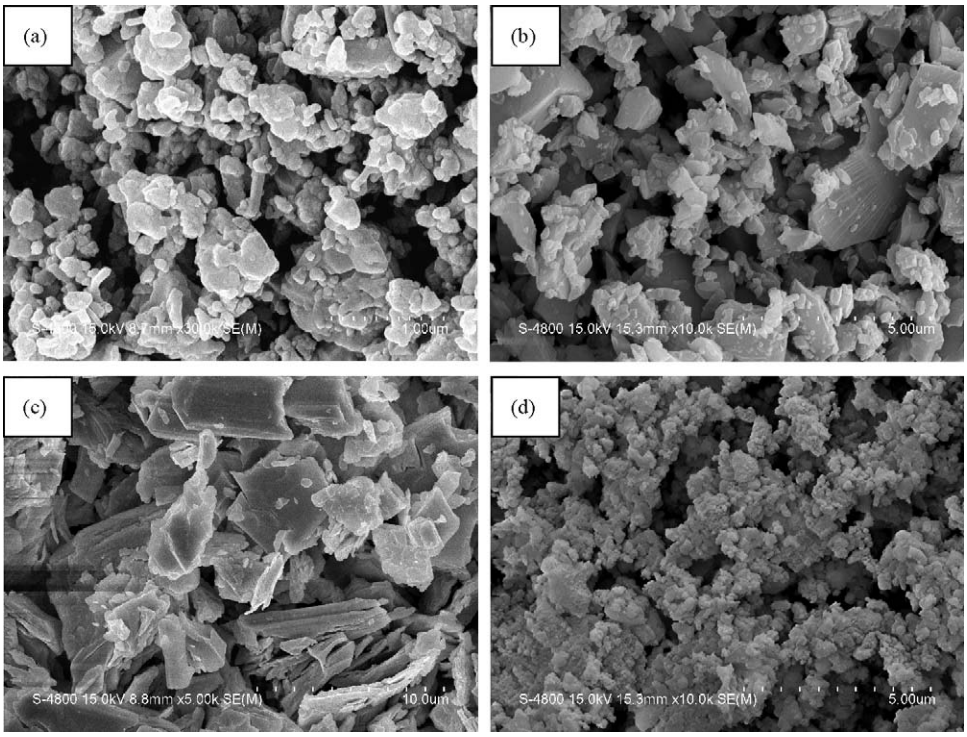

Fig. 1. The microstructure of raw materials: (a) Si_3N_4, (b) SiO_2, (c) Yb_2O_3 and (d) Al_2O_3.

by mechanical stirring till solids loading up to 45 vol.%. Afterwards, the mixtures were milled for 24 h in a nylon resin jar using alumina ball-milling media to break down agglomerates and to achieve good homogeneity. After degassing for 8–10 min in a rotary evaporator under vacuum, the initiator and catalyst were applied to the slurry. Then it was cast into metal mould at room temperature. The mould was kept at temperature of 60–80 °C, and the consolidation of suspension formed a green body. After consolidation, the green bodies were demolded and dried under controlled humidity to avoid cracking and non-uniform shrinkage due to rapid drying. Binder burnout was carried out at 600 °C for 2 h, with a heating rate of 2 °C/min and a natural cooling. Then the samples were embedded in 50 wt.% Si_3N_4 + 40 wt.% BN + 10 wt.% Al_2O_3 powder bed in a graphite crucible and sintered to the temperature of 1680 °C for 1.5 h in N_2 atmosphere, followed by natural cooling under N_2 gas atmosphere.

2.3. Specimen preparation

The thermal shock resistance was determined by measuring the flexural strength of water-quenched specimen. Specimens were machined into a bar shape with dimensions of 3 mm × 4 mm × 36 mm. The bars were ground with a diamond wheel and polished using diamond pastes. The final diamond lap had an abrasive particle of size 3 μm before fracture strength testing and the specimen edges were slightly beveled on a 1200-grit emery paper to remove notches introduced in the course of machining.

2.4. Thermal shock experiments

The thermal shock resistance was carried out in a vertical tube furnace at temperatures between 500 and 1400 °C in air. Ground and polished rectangular bars for thermal shock testing were heated to the desired temperatures and held for 30 min in a furnace before quenching by dropping into a bath of the mixture of water and ice.

2.5. Mechanical test and characterization

The flexural strengths of bars after thermal shock were examined at room temperature by three-point flexure test with a span of 30 mm at a loading rate of 0.5 mm/min. Six samples

Table 1
Raw materials for the AM-MBAM system.

Function	Raw material	Manufacturer
Monomer	Acrylamide (AM)	Aldrich, USA
Crosslinker	*N*,*N*′-Methylenebisacrylamide (MBAM)	Hongxing Biological and Chemical Factory of Beijing, China
Catalyst	*N*,*N*,*N*′*N*′-Tetramethylethylenediamine (TEMED)	Beijing Chemical Reagent Company, China
Initiator	Ammonium persulphate (APS)	Beijing Third Reagent Works, China
Dispersant	Tetramethylammoniumhydoxide solution	Beijing Chemical Reagent Company, China
Solvent	Deionized water	

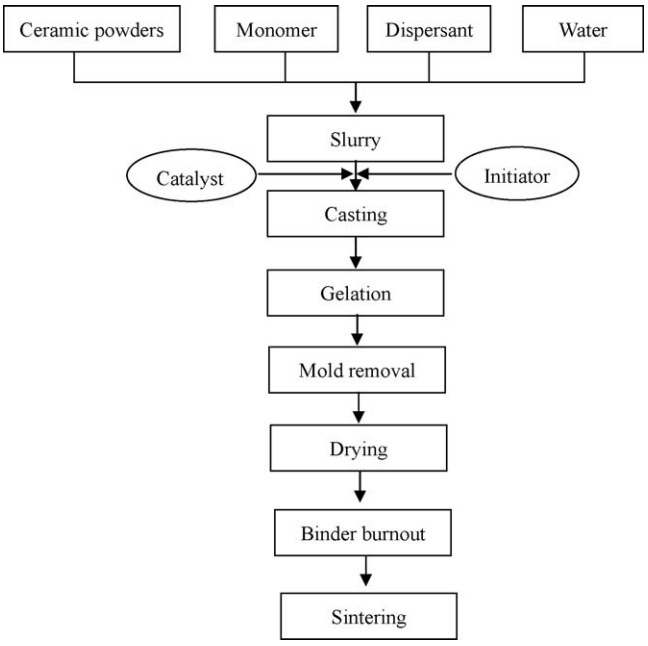

Fig. 2. The gelcasting process flow chart.

were used to calculate the average values and dispersion. Young's modulus was measured by using the pulse echo method. To identify the phase of the samples, XRD (Cu Kα, D/MAX-250, Rigaku, Japan) technique was employed on the polished surfaces. Meanwhile, microstructure analysis of the surfaces of the samples, which were polished with diamond pastes and etched with melting NaOH at 400 °C for 1.5 min, was carried out by scanning electron microscopy (SEM). The porosity of the sample was measured by the mercury porosimetry. The microstructure, pore size, pore distribution and morphology of the fibers in the porous Si_2N_2O–Si_3N_4 bodies of the cross-section were also observed by SEM.

3. Results and discussion

3.1. The Si_2N_2O phase formation

Fig. 3 showed the XRD profiles of the sample. It could be revealed that Si_3N_4 as well as Si_2N_2O phases were all existed. It was the reaction between Si_3N_4 and SiO_2 according to:

$$SiO_2(l) + Si_3N_4(s) \rightarrow 2Si_2N_2O(s) \quad (1)$$

It is thermodynamically possible to form Si_2N_2O from SiO_2 and α-Si_3N_4 or β-Si_3N_4 according to the reaction. The formation of Si_2N_2O indeed proceeds in a liquid phase. The Si_2N_2O crystal structure is built up by distorted [SiN_3O] tetrahedral, whereas α- and β-Si_3N_4 are composed of [SiN_4] tetrahedron is replaced by an oxygen atom, a tetrahedral [SiN_3O] structural unit of Si_2N_2O is formed. Therefore, the Si_2N_2O nuclei are formed in the liquid phase at the sintering temperature. After the Si_2N_2O nucleation occurs, Si_2N_2O grain-growth rate is very high. Si_2N_2O grew via a solution-precipitation process in the presence of a large amount of SiO_2-rich liquid phase. Obviously, the liquid phases were largely consumed with the formation of the crystalline Si_2N_2O.

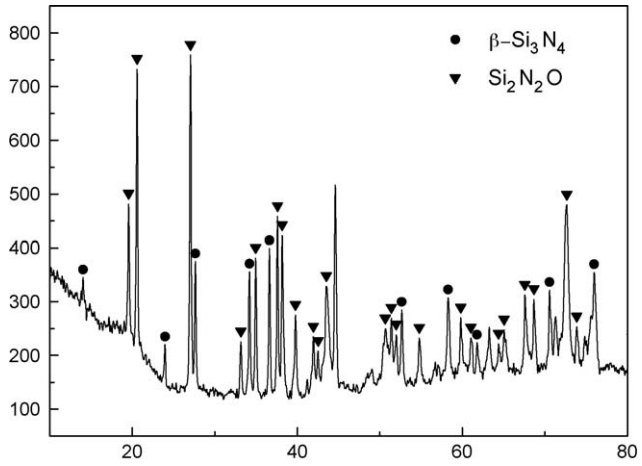

Fig. 3. The XRD profiles of the sample.

3.2. The thermal shock resistance

To evaluate the thermal stress crack initiation and propagation behavior of ceramics, two thermal shock resistance parameters are usually used. According to the theory of critical stress by Kingery [13], the residual strength of material after water quenching is an important index of the thermal shock resistance. Thermal stress fracture resistance parameter R is introduced to estimate thermal stress fracture resistance of materials:

$$\Delta T_{\max} = R = \sigma_f \frac{(1-\upsilon)}{E\alpha} \quad (2)$$

where σ_f is the flexural strength, υ is the Poisson ratio, E is the Young's modulus of elasticity, α is the coefficient of thermal expansion.

Hasselman [14] proposed that the driving force for crack propagation is provided by the elastic energy stored at cracks. The thermal stress damage resistance parameter, R^{IV}, represented by

$$R^{IV} = \frac{E\gamma_f}{\sigma^2(1-\upsilon)} \approx \frac{(K_{IC}/\sigma)^2}{(1-\upsilon)} \quad (3)$$

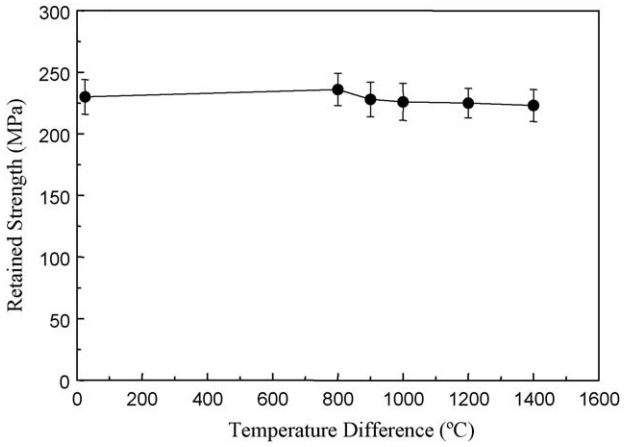

Fig. 4. Flexural strength of Si_2N_2O–Si_3N_4 ceramic after thermal shock with temperature difference (ΔT).

where γ_f is the fracture surface energy and K_{IC} is the fracture toughness. R^{IV} decides the resistance to catastrophic crack propagation of ceramics under a critical temperature difference.

According to the above two equations, it can be clearly seen that the thermal shock resistance can be improved by the increase of the flexural strength and fracture toughness or decrease of Young's modulus and coefficient of thermal expansion.

In the current work, the thermal shock resistance was observed by measuring the flexural strength after thermal shock test, as shown in Fig. 4. It is well known that the traditional thermal shock behavior of monolithic Si_3N_4 is as one of the brittle materials [15]. That is, the flexural strength decreases rapidly after thermal shock with temperature difference. However, the flexural strength of Si_2N_2O–Si_3N_4 ceramic after thermal shock test was not changed much, showing the excellent thermal shock resistance. Moreover, there was no critical temperature (ΔT), at which the strength decreases catastrophically, up to 1400 °C.

3.3. The microstructure and discussion

The excellent thermal shock property of the in situ Si_2N_2O–Si_3N_4 ceramic could be explained as follows.

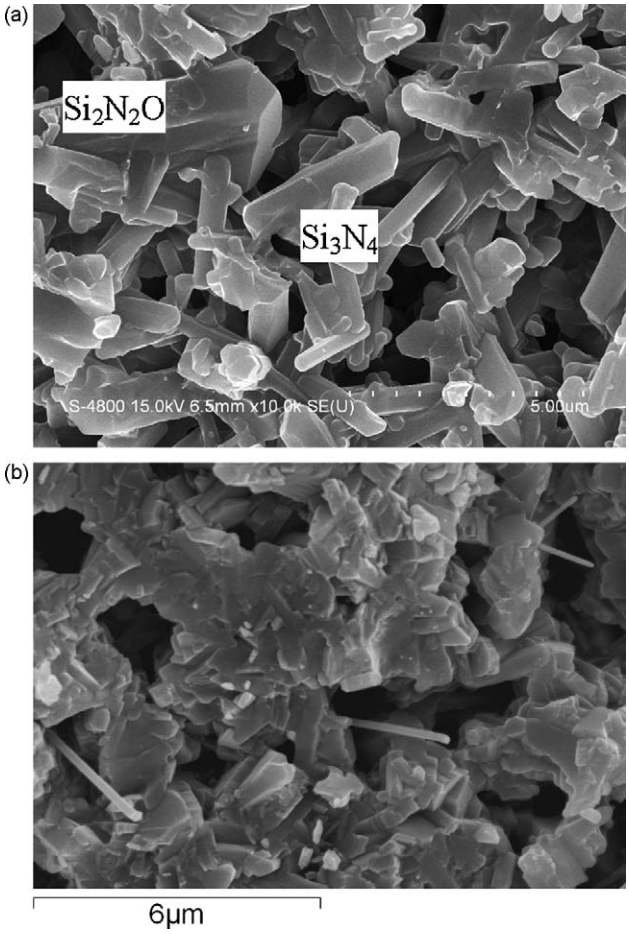

Fig. 5. SEM photograph of the Si_2N_2O–Si_3N_4 composites (a) surface and (b) cross-section.

Firstly, the most important reason for the improving resistance of the materials was the formation of in situ Si_2N_2O which dispersed in silicon nitride matrix ceramics. Fig. 5(a) showed SEM photograph of surface of the Si_2N_2O–Si_3N_4 composites. The composites were comprised of rod β-Si_3N_4 and plate Si_2N_2O phases. Compared to Si_3N_4 ceramics (The Young's modulus was 280 GPa), Si_2N_2O–Si_3N_4 composites possessed low Young's modulus E, which was 125 GPa and the fracture toughness could be improved when the Si_2N_2O dispersed in the β-Si_3N_4 matrix grains [12]. So due to the Si_2N_2O phase, the change trends of the mechanical properties improved the thermal shock resistance of in situ Si_2N_2O–Si_3N_4 composites.

Secondly, the residual pores had great influence on the thermal shock resistance of composites. Fig. 5(b) showed SEM photograph of cross-section of the Si_2N_2O–Si_3N_4 composites. It could be seen that there existed amount of pores that distributed evenly in the matrix and the diameters of the pores were about 3 μm and the porosity was 27%. The pores in composites could be distributed to act as crack stoppers. The thermal shock resistance of ceramics was improved greatly due to the porosity. In the porous microstructure, the irregular shaped Si_2N_2O fibers extended from the pores. The diameters of the Si_2N_2O fibers were about 50–100 nm. Some Si_2N_2O fibers showed wavy and rough surface due to the formation of several nucleation sites. The fibers extended from the pores dissipated the energy of crack growth and contributed to the improvement of the thermal shock property.

4. Conclusion

In this study, the in situ Si_2N_2O–Si_3N_4 composites were prepared via gelcasting and pressureless sintering. The Si_2N_2O–Si_3N_4 composites had excellent thermal shock resistance and the critical temperature difference (ΔT_c) can be up to 1400 °C. The excellent thermal shock resistances were attributed to the Si_2N_2O phase which dissipated the energy of crack growth, and the residual pores and the fibers extended from the pores acted as a stopper to the crack.

References

[1] Y. Inagaki, O.T. Kondon, High performance porous silicon nitrides, J. Eur. Ceram. Soc. 22 (2002) 2489–2494.
[2] Y. Ohji, T. Shigegaki, S. Miyajima, Kanzaki, Fracture resistance behavior of multilayered silicon nitride, J. Am. Ceram. Soc. 80 (1997) 991–994.
[3] J.H. She, J.F. Yang, D.D. Jayaseelan, N. Kondo, T. Ohji, S. Kanzaki, Y. Inagaki, Thermal shock behavior of isotropic and anisotropic porous silicon nitride, J. Am. Ceram. Soc. 86 (2003) 738–740.
[4] S.K. Lee, J.D. Moretti, M.J. Readey, B.R. Lawn, Thermal shock resistance of silicon nitrides using an indentation-quench test, J. Am. Ceram. Soc. 85 (2002) 279–281.
[5] T. Sekine, Shock synthesis of cubic silicon nitride, J. Am. Ceram. Soc. 85 (2002) 113–116.
[6] D.S. Fox, E.J. Opila, Q.N. Nguyen, D.L. Humphrey, S.M. Lewton, Para-linear oxidation of silicon nitride in a water–vapor/oxygen environment, J. Am. Ceram. Soc. 86 (2003) 1256–1261.
[7] M. Backhaus-Ricoult, V. Guerin, A.M. Huntz, V.S. Urbanovich, High-temperature oxidation behavior of high-purity alpha-, beta-, and mixed silicon nitride ceramics, J. Am. Ceram. Soc. 85 (2002) 385–392.

[8] Y. Zhang, Y.B. Cheng, S. Lathabai, K. Hirao, Erosion response of highly anisotropic silicon nitride, J. Am. Ceram. Soc. 88 (2005) 114–120.
[9] A. Zerr, M. Kempf, M. Schwarz, E. Kroke, M. Goken, R. Riedel, Elastic moduli and hardness of cubic silicon nitride, J. Am. Ceram. Soc. 85 (2002) 86–90.
[10] M. Radwan, T. Kashiwagi, Y. Miyamoto, New synthesis route for Si_2N_2O ceramics based on desert sand, J. Eur. Ceram. Soc. 23 (2003) 2337–2341.
[11] X. Rong-Jun, M. Mamoru, X. Fang-Fang, Z. Guo-Dong, B. Yoshio, A. Yoshio, Microstructure and mechanical properties of superplastically deformed silicon nitride–silicon oxynitride in situ composites, J. Eur. Ceram. Soc. 22 (2002) 963–971.
[12] H. Emoto, M. Mitomo, C.M. Wang, H. Hirosturu, T. Inaba, Fabrication of silicon nitride-silicon oxynitride in-situ composites, J. Eur. Ceram. Soc. 18 (1998) 527–533.
[13] W.D. Kingery, Factors affecting thermal stress resistance of ceramic materials, J. Am. Ceram. Soc. 38 (1955) 3–15.
[14] D.P. Hasselman, Elastic energy at fracture and surface energy as design criteria for thermal shock, J. Am. Ceram. Soc. 46 (1963) 535–540.
[15] B. Lee, R.K. Paul, C.W. Lee, H.D. Kim, Fabrication and microstructure characterization of continuously porous Si_2N_2O–Si_3N_4 ceramics, Mater. Lett. 61 (2007) 2182–2186.